

## **Contribution of Genetic Background to the Radiation Risk for Cancer and Non-Cancer Diseases in Ptch1+/- Mice**

Authors: De Stefano, I., Leonardi, S., Casciati, A., Pasquali, E., Giardullo, P., et al.

Source: Radiation Research, 197(1) : 43-56

Published By: Radiation Research Society

URL: <https://doi.org/10.1667/RADE-20-00247.1>

---

BioOne Complete ([complete.BioOne.org](https://complete.BioOne.org)) is a full-text database of 200 subscribed and open-access titles in the biological, ecological, and environmental sciences published by nonprofit societies, associations, museums, institutions, and presses.

Your use of this PDF, the BioOne Complete website, and all posted and associated content indicates your acceptance of BioOne's Terms of Use, available at [www.bioone.org/terms-of-use](https://www.bioone.org/terms-of-use).

Usage of BioOne Complete content is strictly limited to personal, educational, and non - commercial use. Commercial inquiries or rights and permissions requests should be directed to the individual publisher as copyright holder.

---

BioOne sees sustainable scholarly publishing as an inherently collaborative enterprise connecting authors, nonprofit publishers, academic institutions, research libraries, and research funders in the common goal of maximizing access to critical research.

# Contribution of Genetic Background to the Radiation Risk for Cancer and Non-Cancer Diseases in *Ptch1*<sup>+/-</sup> Mice

I. De Stefano,<sup>a</sup> S. Leonardi,<sup>a</sup> A. Casciati,<sup>a</sup> E. Pasquali,<sup>a</sup> P. Giardullo,<sup>a</sup> F. Antonelli,<sup>a</sup> F. Novelli,<sup>a</sup> G. Babini,<sup>b,c,d</sup>  
M. Tanori,<sup>a</sup> B. Tanno,<sup>a</sup> A. Saran,<sup>a</sup> LDLensRad Consortium,<sup>1</sup> M. Mancuso<sup>a,2</sup> and S. Pazzaglia<sup>a,2</sup>

<sup>a</sup> Laboratory of Biomedical Technologies, Agenzia Nazionale per le Nuove Tecnologie, l'Energia e lo Sviluppo Economico Sostenibile (ENEA), Rome, Italy; <sup>b</sup> Department of Physics, University of Pavia, Pavia, Italy; and <sup>c</sup> Department of Woman and Child Health and Public Health, Fondazione Policlinico Universitario A. Gemelli, Istituto di Ricovero e Cura a Carattere Scientifico (IRCCS), Rome, Italy

---

De Stefano, I., Leonardi, S., Casciati, A., Pasquali, E., Giardullo, P., Antonelli, F., Novelli, F., Babini, G., Tanori, M., Tanno, B., Saran, A., LDLensRad Consortium, Mancuso, M. and Pazzaglia, S. Contribution of Genetic Background to the Radiation Risk for Cancer and Non-Cancer Diseases in *Ptch1*<sup>+/-</sup> Mice. *Radiat. Res.* 197, 43–56 (2022).

Experimental mouse studies are important to gain a comprehensive, quantitative and mechanistic understanding of the biological factors that modify individual risk of radiation-induced health effects, including age at exposure, dose, dose rate, organ/tissue specificity and genetic factors. In this study, neonatal *Ptch1*<sup>+/-</sup> mice bred on CD1 and C57Bl/6 background received whole-body irradiation at postnatal day 2. This time point represents a critical phase in the development of the eye lens, cerebellum and dentate gyrus (DG), when they are also particularly susceptible to radiation effects. Irradiation was performed with  $\gamma$  rays (<sup>60</sup>Co) at doses of 0.5, 1 and 2 Gy, delivered at 0.3 Gy/min or 0.063 Gy/min. Wild-type and mutant mice were monitored for survival, lens opacity, medulloblastoma (MB) and neurogenesis defects. We identified an inverse genetic background-driven relationship between the radiosensitivity to induction of lens opacity and MB and that to neurogenesis deficit in *Ptch1*<sup>+/-</sup> mutants. In fact, high incidence of radiation-induced cataract and MB were observed in *Ptch1*<sup>+/-</sup>/CD1 mutants that instead showed no consequence of radiation exposure on neurogenesis. On the contrary, no induction of radiogenic cataract and MB was reported in *Ptch1*<sup>+/-</sup>/C57Bl/6 mice that were instead susceptible to induction of neurogenesis defects. Compared to *Ptch1*<sup>+/-</sup>/CD1, the cerebellum of *Ptch1*<sup>+/-</sup>/C57Bl/6 mice showed increased radiosensitivity to apoptosis, suggesting that differences in processing radiation-induced DNA damage may underlie the opposite strain-related radiosensitivity to

cancer and non-cancer pathologies. Altogether, our results showed lack of dose-rate-related effects and marked influence of genetic background on the radiosensitivity of *Ptch1*<sup>+/-</sup> mice, supporting a major contribution of individual sensitivity to radiation risk in the population. © 2022 by Radiation Research Society

---

## INTRODUCTION

The central aim of radiological protection is to preserve human health from harmful radiation effects. Variation of individual risk for radiation-induced cancer, as well as for the less-investigated non-cancer diseases, is an important concern for the current system and regulations.

Ionizing radiation is frequently referred to as a double-edged sword because while it serves as a pivotal diagnostic and therapeutic tool, it is also a strong genotoxic agent, causing DNA damage and influencing a variety of processes in exposed cells. While most of the evidence on radiation-induced health effects relates to cancer, there has been increasing interest recently in non-cancer diseases, including lens opacity and neurodevelopmental impairment in exposed populations. There is accumulating evidence of the effects of radiation at moderate doses, which include those occurring with lens opacities and in the vascular system (1). As a result, cataract and circulatory diseases were considered as tissue reactions of a stochastic nature, with the threshold considered to be 0.5 Gy, irrespective of the rate of dose delivery (i.e., acute, fractionated/protracted or chronic exposure). For neurodevelopmental impairment, epidemiological studies of childhood brain cancer survivors have shown high doses of ionizing radiation as a well-known risk factor (2–4). The effect of low (below 100 mGy for photon) and moderate doses (between 100 to 2,000 mGy) (5, 6) is still under debate and, given the increased radiation exposure to the general population, research in the low/moderate dose range is critical and represents a priority for radiation protection. Mouse models facilitate exploration

<sup>1</sup> For the LDLensRad Consortium: E. Ainsbury, M. Ahmadi, T. Azizova, F. Antonelli, G. Babini, S. Barnard, C. Dalke, L. Dauer, I. De Stefano, J. Dynlacht, L. Garrett, J. Graw, N. Hamada, S. M. Höflter, M. Jarrin, M. Kadhim, A. Kalligeraki, S. Kunze, S. Leonardi, M. Mancuso, R. McCarron, J. Moquet, D. Pawliczek, S. Pazzaglia, R. Quinlan, A. Saran, R. Tanner, B. Tanno, M. Ung and A. Uwineza.

<sup>2</sup> Address for correspondence: M. Mancuso or S. Pazzaglia: Laboratory of Biomedical Technologies, ENEA Casaccia Research Centre, ENEA Centro Ricerche Casaccia, Via Anguillarese 301, 00123 Rome, Italy; email: mariateresa.mancuso@enea.it; simonetta.pazzaglia@enea.it.

of biological and genetic features that influence the risk of developing diseases after low/moderate-dose irradiation.

The sonic hedgehog (SHH) signaling pathway is important for the organogenesis of almost all organs in mammals, as well as homeostasis during postnatal life and regeneration, including lens (7–9), cerebellum (10) and hippocampal dentate gyrus (DG) (11–13). The SHH pathway signals via two transmembrane proteins, Smoothed (SMO) and its negative regulator, Patched1 (PTCH1). Germ-line mutations in the *PTCH1* gene, the receptor of the SHH pathway, cause the Gorlin syndrome, also known as basal cell nevus syndrome (BCNS), an autosomal dominant disorder distinguished by multi-systemic developmental abnormalities and increased risk of childhood-onset brain tumors. Among BCNS patients, 26% also manifest ocular abnormalities, including cataract in 3–8% of the cases (14, 15). A feature of BCNS patients is tumor abnormal sensitivity to therapeutic doses of ionizing radiation, with development of large numbers of basal cell carcinomas (BCC) in the irradiated skin areas shortly after exposure.

Similarly, *Patched1* heterozygous mice (*Ptch1*<sup>+/-</sup>) are predisposed to BCC and medulloblastoma (MB), a cerebellar tumor, constituting the most common malignant pediatric brain cancer (16, 17), and are prone to patterning defects of the cerebellum and hippocampus (18, 19). Moreover, *Ptch1*<sup>+/-</sup> mice exhibit a marked hypersensitivity to radiation, exhibiting cancer and non-cancer effects. Neonatal irradiation of *Ptch1*<sup>+/-</sup> mice dramatically increases the incidence of BCC and MB (20, 21) and *Ptch1*<sup>+/-</sup> mice are also highly susceptible to cataract induction by radiation exposure in early postnatal age, when lens epithelial cells undergo rapid expansion in the lens epithelium (22, 23).

Tissue reactions and stochastic effects after radiation exposure vary among individuals, and genetic factors are a substantial contributor to individual radiation response. In this study, neonatal *Ptch1*<sup>+/-</sup> mice bred on CD1 and C57Bl/6 background received whole-body irradiation with moderate  $\gamma$ -ray (<sup>60</sup>Co) doses (0.5, 1 and 2 Gy) at a dose rate of 0.3 Gy/min or 0.063 Gy/min on postnatal day 2 (P2). Mice were monitored for survival, development of lens opacity, MB and neurogenesis defects. This neonatal age was selected for exposure as it is a critical phase for development of the eye lens, cerebellum and DG, and therefore particularly susceptible to radiation induced effects. In this study we investigated the dependence of the radiation-induced lens opacity, MB and neurogenesis defects on genetic background, dose rate, and the relationship between induction of lens alterations and other brain cancer and non-cancer pathologies, to establish whether the lens might be predictive of a general brain radiosensitivity. Results showed lack of dose-rate-related effects and marked strain-dependent differences in radiation responses, underlying a critical influence of the genetic background on the radiosensi-

**TABLE 1**  
Summary of the Size of the Experimental Mouse Groups

Treatment		CD1 mice		C57Bl/6 mice	
Dose (Gy)	Dose rate (Gy/min)	No. of wild-type mice	No. of <i>Ptch1</i> <sup>+/-</sup> mice	No. of wild-type mice	No. of <i>Ptch1</i> <sup>+/-</sup> mice
0		11	28	11	22
2	0.063	28	32	34	32
2	0.3	35	26	25	19
1	0.063	16	26	-	-
1	0.3	35	24	-	-
0.5	0.063	23	19	-	-
0.5	0.3	22	18	-	-

tivity of *Ptch1*<sup>+/-</sup> mice both for cancer and non-cancer pathologies, supporting a major contribution of individual sensitivity to radiation risk in the population.

## MATERIALS AND METHODS

### Mice

Mice lacking one *Ptch1* allele were bred on CD1 (named *Ptch1*<sup>+/-</sup>/CD1 throughout the text) or C57Bl/6 (named *Ptch1*<sup>+/-</sup>/C57Bl/6 throughout the text) background and genotyped as described elsewhere (24). Both C57Bl/6/*Ptch1*<sup>+/-</sup> and CD1/*Ptch1*<sup>+/-</sup> mice were generated by breeding the 129S2 mutation for at least 10 generations onto the respective genetic backgrounds. CD1 is an outbred stock, and brother-sister mating was avoided to minimize consanguinity. This animal study was performed according to the European Community Council Directive 2010/63/EU, approved by the local Ethical Committee for Animal Experiments of the ENEA, and authorized by the Italian Ministry of Health (no. 1233/2015-PR).

### Irradiation and Dosimetry

Irradiation of P2 mutant mice and their wild-type (WT) counterparts of both sexes in equal numbers was performed at the Italian National Institute of Ionizing Radiation Metrology (ENEA-INMRI; Rome, Italy) irradiation facility currently used for calibration of radiotherapy dosimeters. All information relative to mice irradiation (dose, dose rate and number) is summarized in Table 1. The beam used was a horizontal <sup>60</sup>Co beam with a field size of 10 cm × 10 cm at 100-cm distance from the source. At the beginning of the irradiation session, the dose rate was 0.16 Gy/min as determined using a reference ionization chamber calibrated in terms of absorbed dose to water with traceability to the Italian primary standard of absorbed dose. Two different dose rates (0.3 Gy/min and 0.063 Gy/min) were obtained varying the source distance at 74.1 and 161.7 cm, respectively. Mice were irradiated in a PMMA holder with 4-mm-thick walls, ensuring electronic equilibrium conditions. The PMMA holder was placed with its midpoint at the source distance realizing the required dose rate within ±

2% and the source distance was changed every four months. The irradiation time ( $t_{irr}$ ) to deliver the required absorbed dose was calculated daily accounting for the <sup>60</sup>Co source decay and according to the formula:

$$t_{irr} = \frac{D}{\dot{D}} - t_{err},$$

where  $D$  is the delivered dose, ( $\dot{D}$ ) is the actual dose rate during irradiation and  $t_{err}$  is the timer error.

The number of mice simultaneously irradiated, established to ensure a beam uniformity within 1%, was  $n = 3$  and  $n = 1$  for the lower and higher dose rate, respectively.

### *Scheimpflug Analysis*

*Ptch1*<sup>+/-</sup> and wild-type mice were examined monthly for lens density using Scheimpflug analysis up to four months postirradiation. Digital images of the lenses and corneas were taken using the OCULUS Pentacam® system (Wetzlar, Germany) as described elsewhere (25). Briefly, after dilation of the pupils with one drop of atropine (0.5%), the mice were held in front of a Scheimpflug camera with the LED light projected into the middle of the pupil. A well-focused image was adjusted with the help of the provided software and by optimizing the distance between the camera and the mouse eye. Evaluation of the images was performed using the Pentacam software. The maximum lens density across the central anterior-posterior lens axis was quantified with the provided “densitometry along a line” tool.

### *Histological Analysis and Tumor Quantification*

Mice were observed daily up to 10 months of age. Upon decline in health (i.e., severe weight loss, paralysis, ruffling of fur or inactivity) or when tumors were visible, animals were sacrificed and autopsied. Whole-brain and any other visible masses were partly fixed in 10% buffered formalin and partly snap frozen. Samples were then embedded in paraffin wax, sectioned and stained according to standard techniques. Tumor incidence was expressed as the percentage of mice with one tumor.

### *Analysis of Hippocampal Neurogenesis*

For general morphometric analyses, *Ptch1*<sup>+/-</sup> mice ( $n = 4/5$ ), were sacrificed via cervical dislocation at six weeks postirradiation and brains were fixed in 10% buffered formalin and embedded in paraffin wax for histological analysis. To determine DG length, serial sagittal sections were sampled every 100  $\mu\text{m}$  through the whole cerebral hemispheres. Dentate gyrus and brain lengths were measured in each section and the mean values were expressed as the arithmetic means measured out of 3–5 mice. For normalization, DG length was divided for the maximum length of cross-sectional brain. For morphometric

analyses, NIS-Elements BR 4.00.05 imaging software (Nikon Instruments Europe B.V., Italy) was used.

### *Immunohistochemistry*

Fixed tissue sections were immunostained as described elsewhere (26) using the following primary antibodies diluted as indicated by the manufacturer: Sox2 (Abcam, Cambridge, UK), DCX (Abcam) and cleaved caspase-3 (Cell Signaling, Danvers, MA). Cell quantification was performed on collected sections (stained for Sox2 and DCX) using the aforementioned imaging software NIS-Elements. The number of positive cells in the subgranular zone (SGZ) was expressed per  $\mu\text{m}$  of the SGZ length. NSCs were counted based on criteria including SGZ localization, positive labeling and morphology.

### *Quantification of Apoptosis in the Cerebellum*

Brains ( $n = 3/4$ ) from irradiated and age-matching nonirradiated pups were collected at 4 h postirradiation and fixed in 10% buffered formalin. Serial sections of cerebellar tissues were cut at 4- $\mu\text{m}$  thickness and labeled by caspase-3. Digital images from midsagittal cerebellar sections, covering the entire EGL, were collected by IAS image-processing software (Delta Sistemi, Rome, Italy). Intensity measurement of anti-caspase-3 immunohistochemical staining has been performed using HistoQuest 2.0.2.0249 software (TissueGnostic, Vienna, Austria).

### *Statistical Analysis*

Scheimpflug images were analyzed through evaluation of the maximum lens density followed by a linear regression curve fit (95% CI; best-fit value using two parameters: y-intercept and slope). Kaplan-Meier survival curves were compared, and log-rank test  $P$  values were calculated. IHC scoring, intensity and morphometrics are reported as means  $\pm$  SD, and two-tailed Student's  $t$  test was used for determination of statistical difference between groups.  $P \leq 0.05$  was considered statistically significant. Analyses were performed using GraphPad Prism version 5.0 for Windows (San Diego, CA).

## RESULTS

### *Survival of Newborn *Ptch1*<sup>+/-</sup> and Wild-Type Mice on CD1 or C57Bl/6 Background after $\gamma$ -Ray Irradiation*

We examined the influence of CD1 and C57Bl/6 genetic backgrounds on survival of nonirradiated and irradiated wild-type and *Ptch1*<sup>+/-</sup> mouse populations (Fig. 1). While the survival of nonirradiated *Ptch1*<sup>+/-</sup>/CD1 mice was comparable to that of wild-type mice (Fig. 1A), mouse mortality in *Ptch1*<sup>+/-</sup>/C57Bl/6 mice was increased compared to wild-type mice ( $P = 0.005$ ; Fig. 1B). A striking increase in mortality was observed in *Ptch1*<sup>+/-</sup>/CD1 mice that were exposed to 2 Gy of  $\gamma$ -ray radiation at

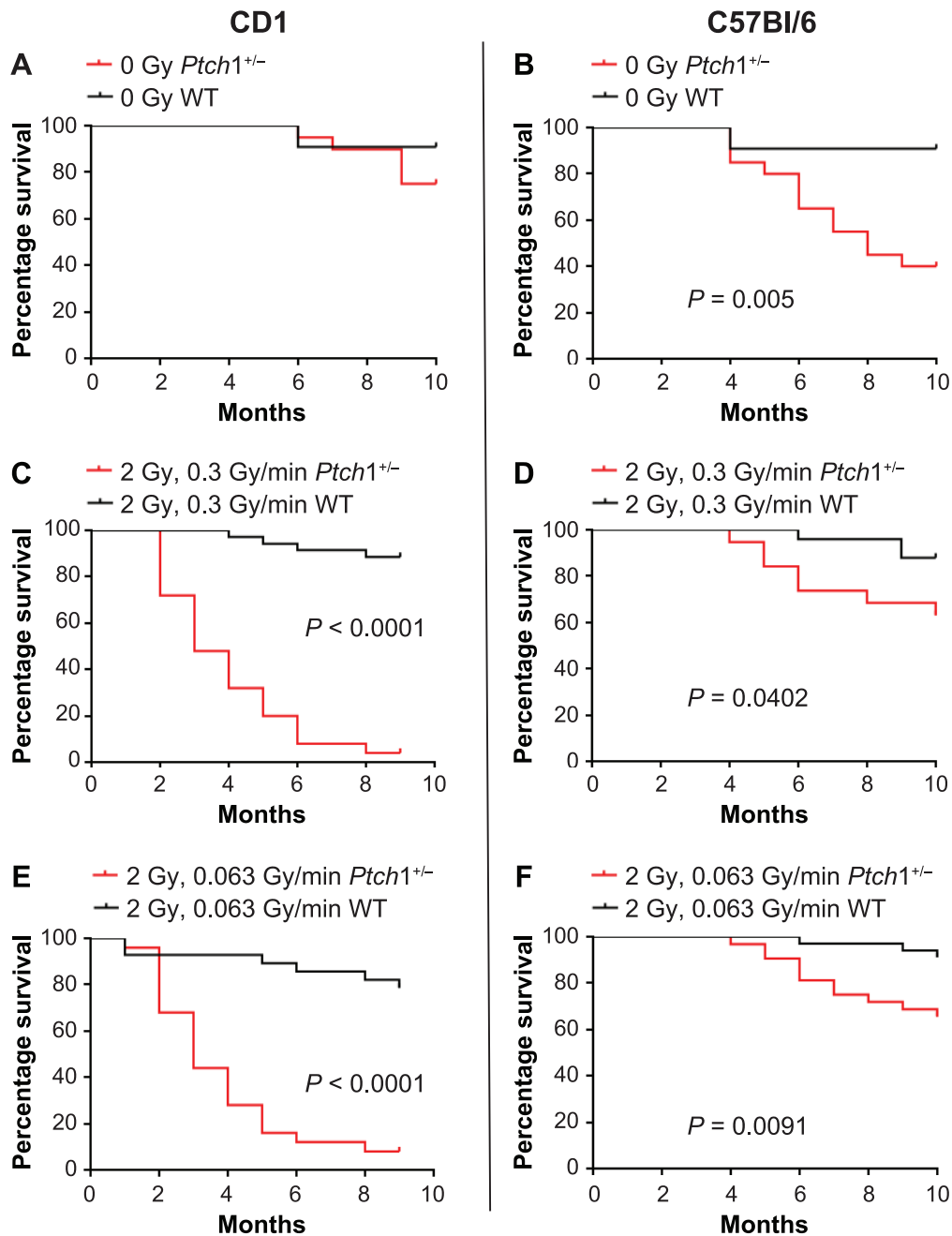


**FIG. 1.** Genetic background and dose-rate effects on mouse survival. Mortality of nonirradiated wild-type (WT) and *Ptch1*<sup>+/-</sup> mice on a CD1 (panel A) or C57Bl/6 (panel B) background, of WT and *Ptch1*<sup>+/-</sup>/CD1 mice that received 2 Gy  $\gamma$ -ray irradiation at 0.3 Gy/min (panel C) or 0.063 Gy/min (panel E) and of WT and *Ptch1*<sup>+/-</sup>/C57Bl/6 mice that received 2 Gy  $\gamma$ -ray irradiation at 0.3 Gy/min (panel D) or 0.063 Gy/min (panel F).

0.3 Gy/min or 0.063 Gy/min ( $P < 0.0001$ ; Fig. 1C and E). In contrast, although increased mortality was observed in 2 Gy irradiated *Ptch1*<sup>+/-</sup>/C57Bl/6 mice at both dose rates compared to wild-type C57Bl/6 mice ( $P = 0.0402$  at 0.3 Gy/min;  $P = 0.0091$  at 0.063 Gy/min; Fig. 1D and F), this mortality was comparable to that of nonirradiated *Ptch1*<sup>+/-</sup>/C57Bl/6 mice ( $P = 0.256$  at 0.3 Gy/min;  $P = 0.108$  at 0.063 Gy/min), confirming that mouse radiosensitivity is strongly dependent on genetic background hosting the *Ptch1*<sup>+/-</sup> mutation.

#### *MB Tumorigenesis after Irradiation of Newborn *Ptch1*<sup>+/-</sup> Mice on CD1 or C57Bl/6 Background*

We have previously demonstrated that X-ray irradiation of newborn *Ptch1*<sup>+/-</sup>/CD1 mice at different doses (0.89 Gy/min) dramatically increased MB incidence (20, 27). Here we show that irradiation of *Ptch1*<sup>+/-</sup>/CD1 mice significantly increased MB incidence either at 0.3 Gy/min (0/28 vs. 20/26, 76.92%;  $P < 0.0001$ ) or at 0.063 Gy/min (0/28 vs. 22/32, 68.75%;  $P < 0.0001$ ) (Fig. 2A–C). However, despite

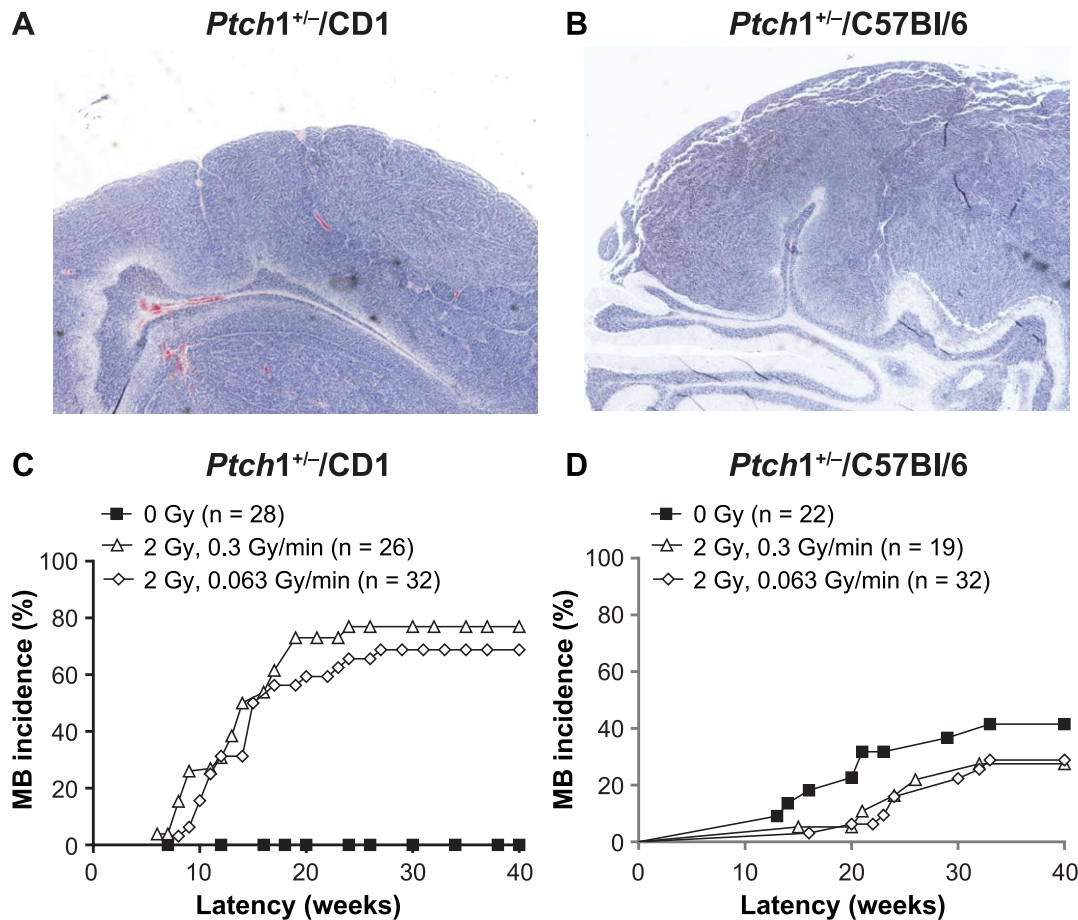


**FIG. 2.** Genetic background effects on medulloblastoma (MB) induction. Panels A and B: Histological features of MB in *Ptch1*<sup>+/-</sup>/CD1 and *Ptch1*<sup>+/-</sup>/C57Bl/6 irradiated mice, respectively. Panels C and D: Spontaneous and radiation-induced MB incidences in *Ptch1*<sup>+/-</sup>/CD1 and *Ptch1*<sup>+/-</sup>/C57Bl/6 mice, respectively.

the significantly higher spontaneous MB incidence in *Ptch1*<sup>+/-</sup>/C57Bl/6 mice compared to *Ptch1*<sup>+/-</sup>/CD1 mice [9/22 (40.9%) vs. 0/28 (0%);  $P = 0.0002$ ], 2 Gy  $\gamma$  rays did not increase MB incidence over the spontaneous rate in *Ptch1*<sup>+/-</sup>/C57Bl/6 mice either at 0.3 Gy/min (5/19; 26.31%) or 0.063 Gy/min (9/32; 28.12%) (Fig. 2D). Given the resistance of *Ptch1*<sup>+/-</sup>/C57Bl/6 mice to the induction of radiogenic MB at 2 Gy, irradiation at lower doses of 0.5 and 1 Gy has only been performed on *Ptch1*<sup>+/-</sup> and wild-type mice on a CD1 background. Irradiation significantly reduced the survival in only the *Ptch1*<sup>+/-</sup> mice at both doses and dose rates ( $P = 0.0067$  at 0.5 Gy, 0.3 Gy/min;  $P = 0.0001$  at 0.5 Gy, 0.063 Gy/min;  $P < 0.0001$  at 1 Gy at both 0.3 and 0.063 Gy/min), and not in the wild-type CD1 mice (Fig. 3A–D). Again, life-shortening was nearly exclusively due to MB induction as  $\gamma$ -ray irradiation resulted in significantly increased MB incidence over the spontaneous rate either at 0.3 Gy/min (4/18, 22.22% at 0.5 Gy,  $P = 0.018$ ; 18/24, 75% at 1 Gy,  $P < 0.0001$ ) or 0.063 Gy/min (6/19, 31.58% at 0.5 Gy,  $P = 0.0025$ ; 15/26, 57.69% at 1 Gy,  $P < 0.0001$ ), without any significant dose-rate effects on survival or tumor induction (Fig. 3E and F).

Key outputs for tumorigenesis include cancer resistance in *Ptch1*<sup>+/-</sup>/C57Bl/6 mice exposed to a moderate dose of 2 Gy compared to *Ptch1*<sup>+/-</sup>/CD1. Instead, in a CD1 background,  $\gamma$ -ray doses  $\geq 0.5$  Gy significantly induced MB development in *Ptch1*<sup>+/-</sup> mutants. There were no significant effects of dose rate on survival or MB induction in the *Ptch1*<sup>+/-</sup>/CD1 mice. Altogether, the data show that genetic background was the predominant factor in MB development in this study.

#### Induction of Lens Opacity after Irradiation of Neonatal *Ptch1*<sup>+/-</sup> Mice on CD1 or C57Bl/6 Background

As a first step to investigate the contribution of mouse genetic background to cataract radiosensitivity, after eyes opening (between 20 days and 1 month of age), groups of 2 Gy irradiated and nonirradiated *Ptch1*<sup>+/-</sup> and wild-type mice on a CD1 or C57Bl/6 background were checked for the presence of macroscopic cataract (Fig. 4A), histologically confirmed (Fig. 4B). Results showed complete resistance to induction of macroscopically visible cataract when radiation was delivered to C57Bl/6 mice, irrespective of *Ptch1* status (0/25 vs. 0/19 at 0.3 Gy/min; 0/34 vs. 0/32 at 0.063 Gy/min,

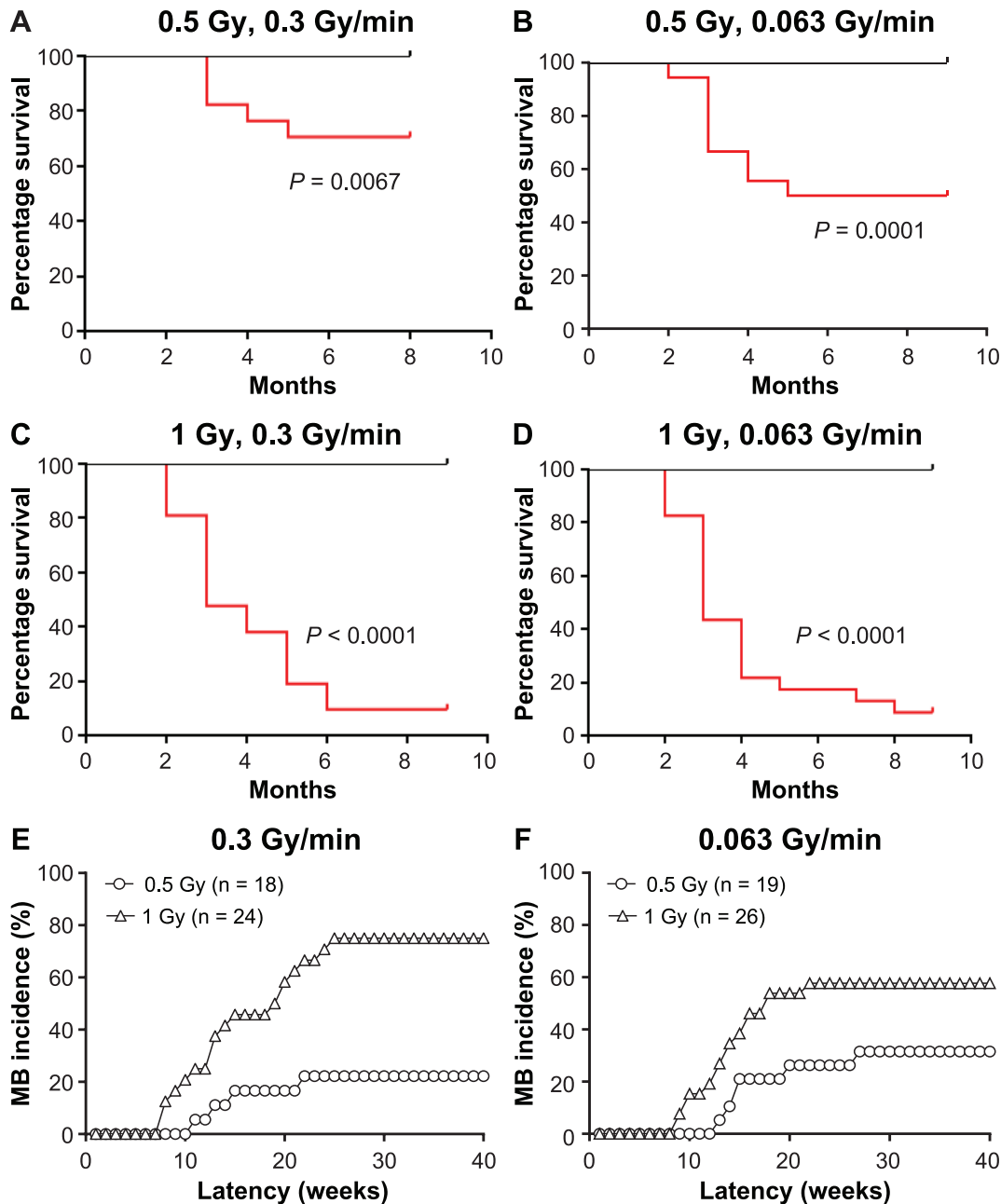


**FIG. 3.** Dose and dose-rate effects on survival and MB tumorigenesis in *Ptch1*<sup>+/</sup>/CD1 mice. Mortality of WT and *Ptch1*<sup>+/</sup>/CD1 mice  $\gamma$ -ray irradiated with 0.5 Gy at 0.3 Gy/min (panel A) or 0.063 Gy/min (panel B) or with 1 Gy at 0.3 Gy/min (panel C) or 0.063 Gy/min (panel D). Radiation-induced MB incidences in *Ptch1*<sup>+/</sup>/CD1 mice irradiated with 0.5 or 1 Gy at 0.3 Gy/min (panel E) or 0.5 or 1 Gy at 0.063 (panel F).

data not shown). In contrast, while the increase of cataract in 2 Gy irradiated wild-type CD1 mice was not significant compared to wild-type C57Bl/6 mice (3/35 vs. 0/25 at 0.3 Gy/min,  $P = 0.26$ ; 2/28 vs. 0/34 at 0.063 Gy/min,  $P = 0.20$ ), it was highly significant in *Ptch1*<sup>+/</sup>/CD1 compared to *Ptch1*<sup>+/</sup>/C57Bl/6 mice (8/25 vs. 0/19 at 0.3 Gy/min,  $P = 0.0065$ ; 16/31 vs. 0/32 at 0.063 Gy/min,  $P = 0.0001$ ; Fig. 4C). The increased incidence of cataract in 2 Gy irradiated *Ptch1*<sup>+/</sup>/CD1 mice was also significant compared to 2 Gy irradiated wild-type CD1 mice (8/25 vs. 3/35 at 0.3 Gy/min,

$P = 0.0392$ ; 16/31 vs. 2/28 at 0.063 Gy/min,  $P = 0.0002$ ), confirming a critical role for the *Ptch1* gene in protecting mouse lens from cataract in the CD1 background.

Lens transparency requires the orderly arrangement of lens cells, and high density and close packing of their protein constituents, primarily the lens crystallins. Changes in lens microarchitecture, protein constituents, or both can result in variation in the refractive index and, thus, light scattering (28). To further investigate lens injury we assessed the presence of opacification by measuring lens

density monthly using Scheimpflug imaging between 1–4 months of age (Fig. 4D) since, beyond this age, survival of irradiated *Ptch1*<sup>+/-</sup>/CD1 mice sharply decrease for MB. The Scheimpflug analysis data, plotted as maximum lens density against the month of examination, clearly showed a higher density in nonirradiated CD1 compared to C57Bl/6 mice (10 vs. 6.4;  $P < 0.0001$ ; Fig. 4D), highlighting important background-related differences in the basal level of lens density. In both strains, *Ptch1* heterozygosity did not modify lens density without irradiation at all months examined (Fig. 4E). In CD1 mice, radiation increased maximum lens density by approximately twofold (from 10 to 18.1 at 1 month for 0.3 Gy/min,  $P = 0.0124$ ; 20.7 for 0.063 Gy/min,  $P = 0.037$ ) in wild-type mice and even more robustly in *Ptch1*<sup>+/-</sup>/CD1 mice (from 10 to 41 at 1 month for 0.3 Gy/min,  $P < 0.0001$ ; 49 for 0.063 Gy/min,  $P < 0.0001$ ), greatly exceeding the LOCS III criteria of 14 for visual impairment (29) (Fig. 4F and G). No substantial differences in the increase of maximum cell density were observed between the two dose rates in either wild-type or *Ptch1*<sup>+/-</sup>/CD1 mice. Opacification progressively increased with time in *Ptch1*<sup>+/-</sup>/CD1 mice at both dose rates, with maximum lens density at 4 months reaching values of 59 at 0.3 Gy/min and 62 at 0.063 Gy/min. In marked contrast, no radiation-dependent increase of maximum lens density after irradiation was observed in either C57Bl/6 wild-type or *Ptch1*<sup>+/-</sup>/C57Bl/6 mice at either dose rate.

On the whole, the data showed that irradiation of mice at P2 dramatically accelerates cataractogenesis in wild-type mice and *Ptch1*<sup>+/-</sup>/CD1 mice, but not in C57Bl/6 mice, in which cataract development was completely abrogated regardless of the *Ptch1* status, demonstrating an opposite radiosensitivity of the CD1 and C57Bl/6 backgrounds to induction of radiogenic lens opacity. Therefore, these results showed that the genetic background significantly alters the risk for cataract and, importantly, suggest that the interactions between genetic and modifying factors are able to completely abrogate the induction of lens opacification also in the presence of a penetrant germline gene mutation representing a paradigm for radiation hypersensitivity, such as *Ptch1* heterozygosity.

#### *Neurogenesis after Irradiation of Newborn Ptch1*<sup>+/-</sup> Mice on CD1 or C57Bl/6 Background

Neurogenesis refers to the entire set of events leading to the production of new neurons from precursor cells in the brain (Fig. 5B) (30). Dentate gyrus neurogenesis is regulated by multiple intrinsic and extrinsic factors that control neural stem cell (NSC) proliferation, maintenance, and differentiation into mature neurons. Radiation negatively affects neurogenesis and, while cranial irradiation can effectively treat brain tumors, it may also cause cognitive impairments through the disruption of hippocampal neurogenesis, especially at young age (31–33, 26). We here investigated the consequence of 2 Gy  $\gamma$ -ray irradiation at

P2, a critical age during the developmental timeline for DG, on hippocampal neurogenesis in *Ptch1*<sup>+/-</sup> mutants (Fig. 5A). We focused on genetic background-related aspects, analyzing subclasses of progenitor cells and newborn neurons in the DG of *Ptch1*<sup>+/-</sup> mutants on CD1 and C57Bl/6 background at six weeks postirradiation. To measure the neurogenesis rate we adopted criteria based on a combination of morphological cellular features and immunohistochemical labeling with stage-specific adult neurogenesis markers, measuring transient amplifying progenitor cells (sex determining region Y (SRY) box 2 (Sox2)<sup>+</sup>, and immature granule neurons [doublecortin (DCX)<sup>+</sup>] (Fig. 5B). Results showed no significant consequences of 2 Gy P2 irradiation in *Ptch1*<sup>+/-</sup>/CD1 mice at six weeks postirradiation (Fig. 5C and D). Instead, in the *Ptch1*<sup>+/-</sup>/C57Bl/6 mice irradiation significantly impaired both Sox2<sup>+</sup> progenitors (0.0026 vs. 0.038,  $P = 0.0088$ ) and DCX<sup>+</sup> newborn neuron populations (0.047 vs. 0.084,  $P = 0.0069$ ) (Fig. 5C and D), suggesting that the overall sensitivity of neural progenitors of the SGZ of the DG to radiation is strongly exacerbated on a C57Bl/6 genetic background.

#### *Mechanistic Insights into the Dependence of Radiation Effects on Genetic Background in the Cerebellum*

Since results of a DDR-focused miRNome analysis in the lens (object of another manuscript of this special issue) pointed to a marked upregulation of p53 signaling in *Ptch1*<sup>+/-</sup>/C57Bl/6 compared to *Ptch1*<sup>+/-</sup>/CD1 mice at 24 h postirradiation, which are suggestive of persistent DNA damage, we investigated the apoptotic responses in the cerebellum of irradiated *Ptch1*<sup>+/-</sup>/C57Bl/6 and *Ptch1*<sup>+/-</sup>/CD1 mice (Fig. 6). We evaluated the expression of the caspase-3 apoptotic marker in the external granule layer region of the cerebellum, the location of the precursors responsible for most of the postnatal neurogenesis of the cerebellum, also representing the MB cell of origin. The 2 Gy irradiated *Ptch1*<sup>+/-</sup>/C57Bl/6 mice showed significantly higher apoptotic rate (0.205 vs. 0.148;  $P = 0.0311$ ) compared to *Ptch1*<sup>+/-</sup>/CD1 at 4 h postirradiation (Fig. 6A–C) suggesting a higher radiosensitivity to cell killing of the granule precursor population in the cerebellum of C57Bl/6 mice.

## DISCUSSION

In this study, we investigated and correlated the long-term health effects of moderate  $\gamma$ -ray doses at P2, during an extremely susceptible developmental phase of the lens, cerebellum and DG, to genotoxic stress. Neonatal irradiation is relevant to the human situation, as individuals exposed to radiation prenatally and during childhood have a higher risk for acute and long-term radiation effects.

It is well known that the phenotypic consequences of mutation may vary across genetically distinct individuals. Genetic variants contributing to background effects are termed “modifiers” and can dramatically alter the individ-

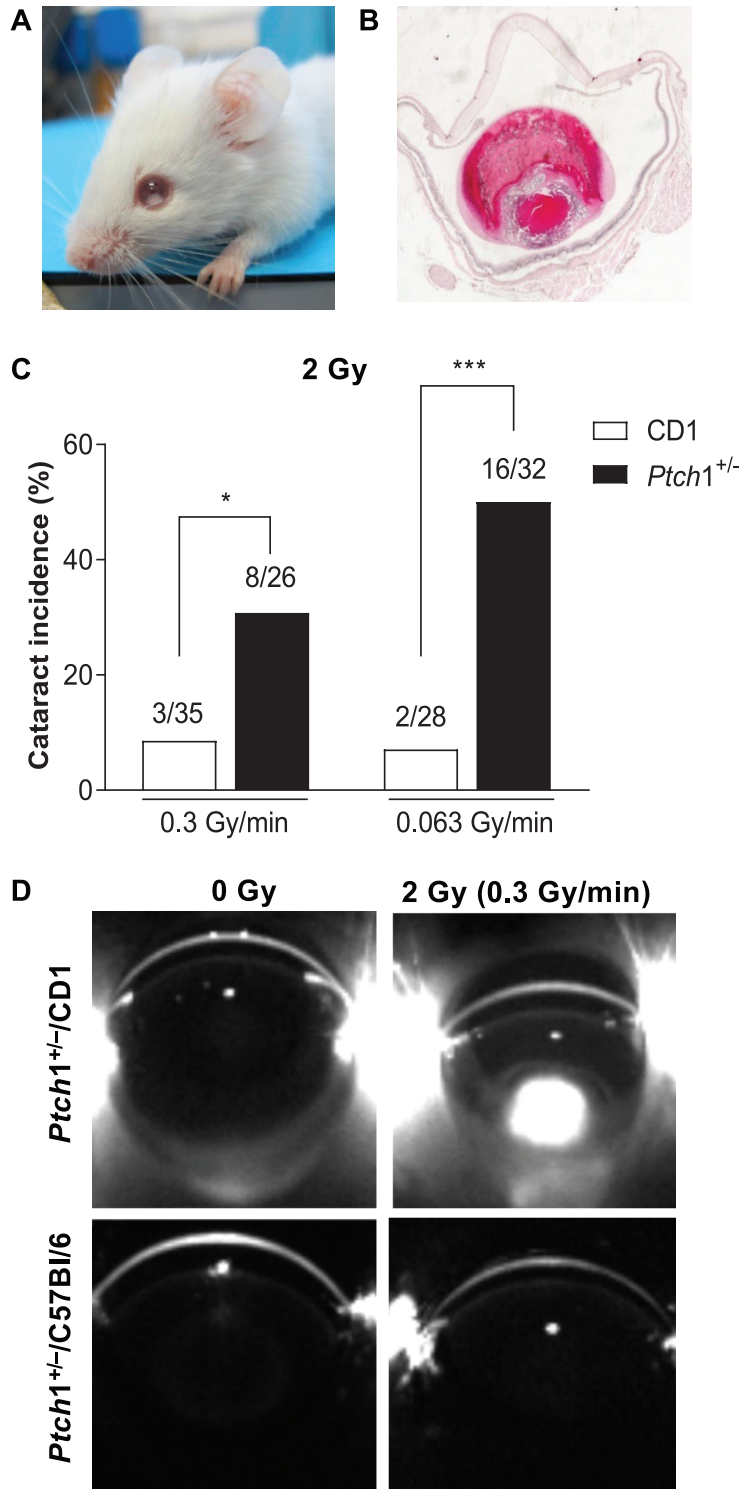


**FIG. 4.** Role of genetic background in controlling the induction of lens opacity in *Ptch1*<sup>+/-</sup> and WT mice irradiated at P2. Panel A: Macroscopically visible cataract is recognizable as a white pinpoint focus in the pink eye. Panel B: Representative histological cataract appearance. Panel C: Incidence of macroscopic cataract in 2 Gy irradiated *Ptch1*<sup>+/-</sup>/CD1 and CD1 WT mice. Panel D: Representative Scheimpflug image of lens from nonirradiated or 2 Gy irradiated *Ptch1*<sup>+/-</sup> mice on a CD1 and C57Bl/6 background. Panel E: Evaluation of lens opacity through Scheimpflug analysis in nonirradiated *Ptch1*<sup>+/-</sup> and WT mice on a CD1 and C57Bl/6 background. Panel F: Evaluation of the effect of 2 Gy P2 irradiation using 0.3 Gy/min on lens opacity through Scheimpflug analysis in *Ptch1*<sup>+/-</sup> and WT mice on a CD1 and C57Bl/6 background. Panel G: Evaluation of the effect of 2 Gy P2 irradiation using 0.063 Gy/min on lens opacity through Scheimpflug analysis in *Ptch1*<sup>+/-</sup> and WT mice on a CD1 and C57Bl/6 background. \**P* < 0.05, \*\*\**P* < 0.0001.

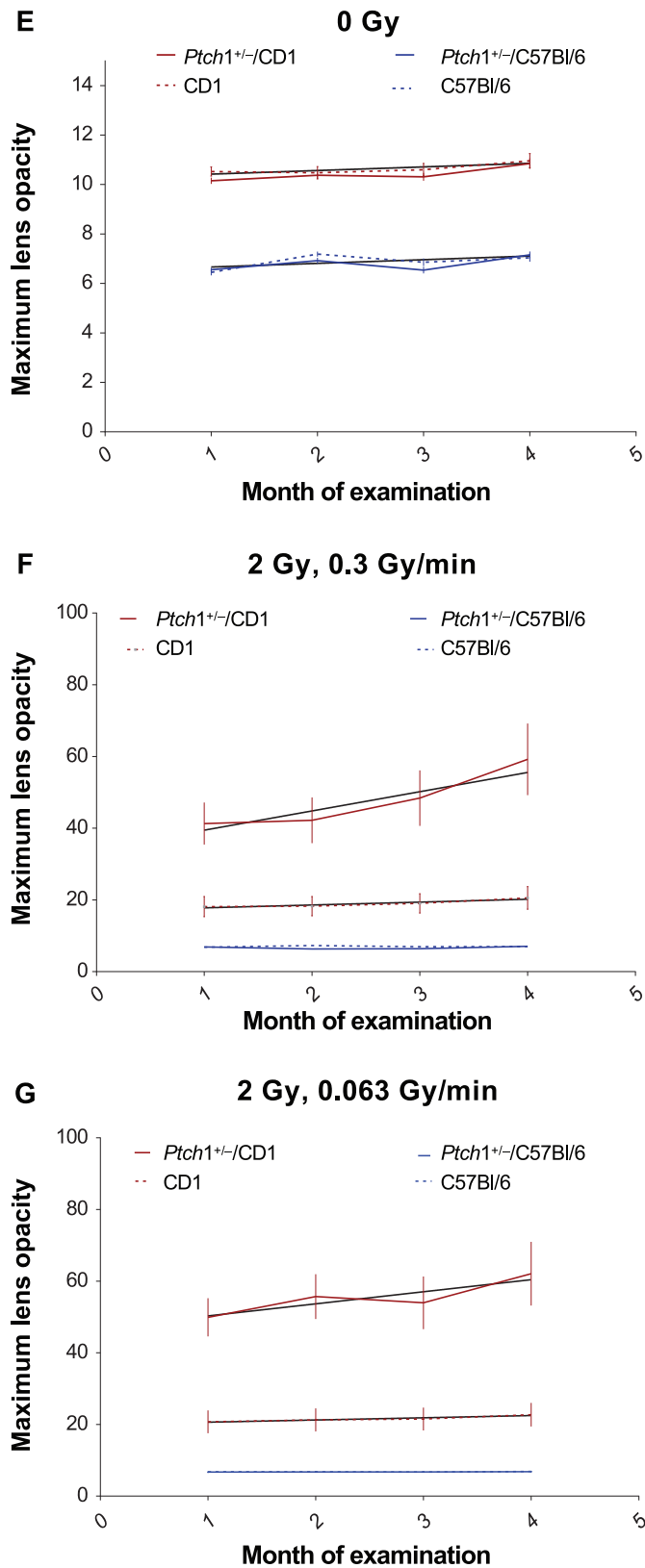
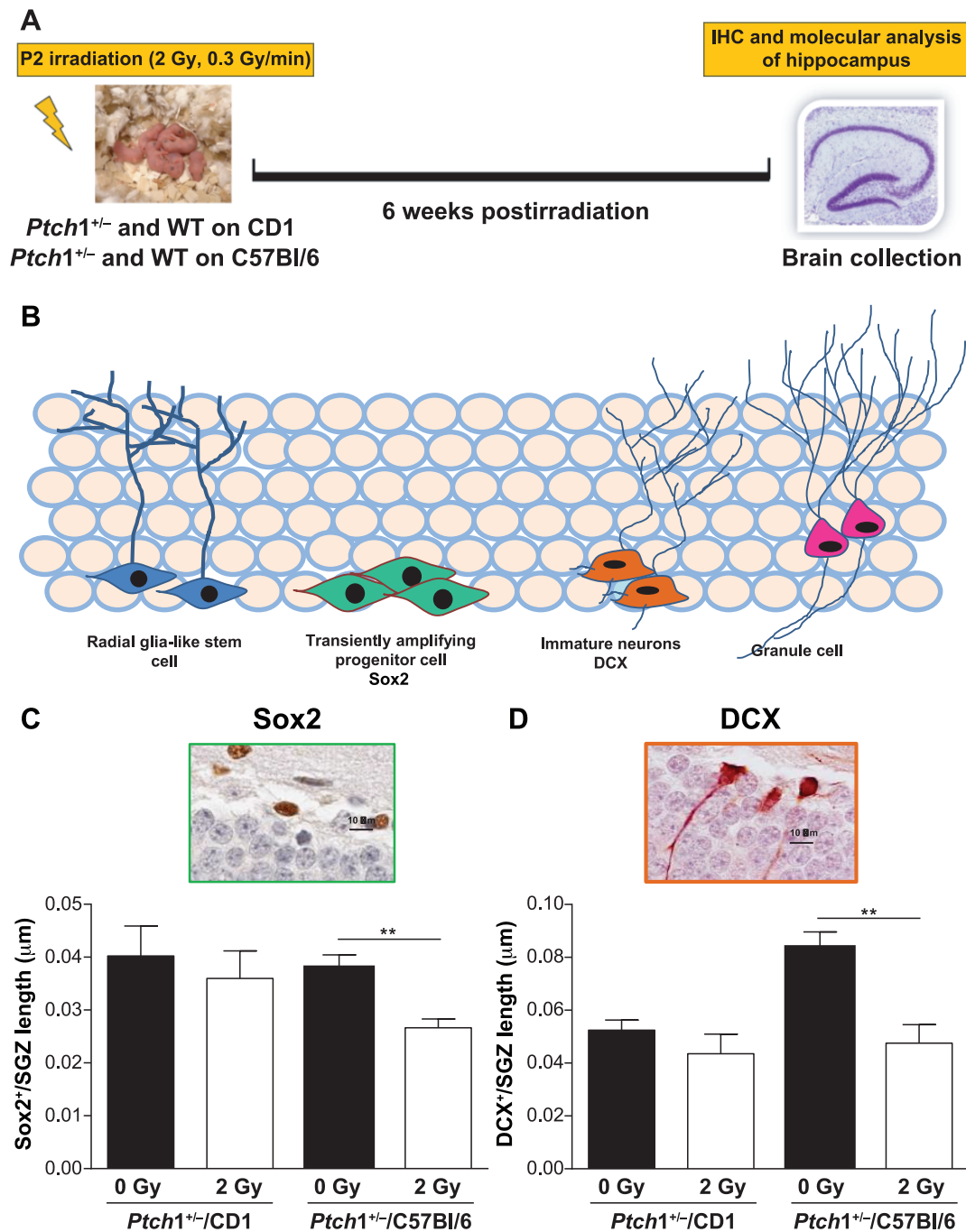


FIG. 4. Continued.

ual risk modulating the phenotype of a given genetic mutations, and/or its interaction with environmental factors including ionizing radiation, complicating our ability to predict individual phenotypes from genetic information. Differences in the magnitude of radiation-induced risks between individuals or groups, relating to genetic make-up, raise very important ethical and policy questions as to whether some individuals/groups are inadequately- or over-protected by the current system and regulations. Individual variation in radiation-related risk for cancer and non-cancer diseases is a key area when addressing radiation protection (34). Improving our understanding of the influence of individual susceptibility on radiation-induced health effects is one of the seven research priorities recommended in the Strategic Research Agenda of the Multidisciplinary European Low Dose Initiative (5) to EU and national funding agencies (<https://bit.ly/3srLIdy>).

The SHH signaling has been demonstrated to play crucial roles in the development of multiple organs, including lens, cerebellum and hippocampus. The SHH pathway is a master player in cerebellar patterning and in regulating and proliferation of precursor cells in the neonatal cerebellum (10) with a concomitant role (when mutated) in cerebellar tumor development. The SHH signaling pathway is essential for many of the steps leading to the formation of a mature ocular primordium (7) and it has been shown to play a role in mouse lens development (8) and in lens regeneration of the adult (9). Emerging findings suggest that the SHH pathway also plays important roles in establishing the hippocampal neurogenic niches in embryo, and it is involved in the formation and plasticity of neuronal circuits in the hippocampus (11–13).

BCNS syndrome shows high penetrance and great inter- and intra-familial phenotypic variability as patients carrying the same mutation can exhibit different clinical symptoms. Similarly, we and others have demonstrated that mouse genetic background hosting the *Ptch1* heterozygous mutation can deeply modify the incidence of *Ptch1*-associated tumors, such as rhabdomyosarcoma, MB and BCC, demonstrating that strain-specific alleles interacting with *Ptch1* heterozygosity modulate tumorigenesis (35–37). Genetic factors might also be important in the pathogenesis of non-cancer diseases, including cataract (38). In fact, significant genetic influence of age-related cortical cataract, with heritability accounting for 53–58% of the liability, has been demonstrated in a published twin eye study (39). Similarly, genetic factors were found to account for approximately 48% of the risk for nuclear cataract (40) and hereditary congenital cataract shows an important intra- and inter-familial variability. Also, adult hippocampal neurogenesis is under complex genetic control, although the environmental influences are also significant. Genetic variation among mouse strains accounted for differences in all aspects of hippocampal neurogenesis, proliferation, survival and differentiation, as well as overall hippocampal volume and total cell numbers (41) showed a significant



**FIG. 5.** Genetic alterations of hippocampal neurogenesis in 2 Gy  $\gamma$ -ray irradiated *Ptch1*<sup>+/-</sup>/CD1 and *Ptch1*<sup>+/-</sup>/C57Bl/6 mice. Panel A: Schematic representation of the experimental design. Panel B: Depiction of the stages of the neurogenic process in the hippocampus. The radial glia-like stem cells (blue) maintain their pool through self-renewal and give rise to transient amplifying progenitor cells (green) expressing similar markers but displaying different morphology, which undergo rapid proliferation; their progeny begin to express DCX (orange), a marker specific to the neuronal fate. Then, the mature granule cells (fuchsia) integrate into the molecular layer. Panels C and D: Quantification of the Sox2-labeled progenitor cells and DCX-labeled newborn neurons, respectively, in the dentate gyrus of nonirradiated and irradiated *Ptch1*<sup>+/-</sup> mice on CD1 or C57Bl/6 background.

correlation between cell survival and neurogenesis, indicating that 85% of the variance in neurogenesis between strains could be accounted for by different cell-survival rates.

Furthermore, several examples of genetic background-related modulation of the penetrance in CD1 vs. C57Bl/6 mouse lines for genes other than *Ptch1* are reported in the

literature. The Noggin null mouse phenotype is strain dependent, leading to embryo lethality at 14.5 dpc in C57Bl/6, but not in CD1 mice, in which lethality manifested at later times and embryos died at perinatal age (42). Background-related differences in the phenotype of the neurological disease dystonia with lethality of 129-*Tor1a*<sup>DEI</sup>

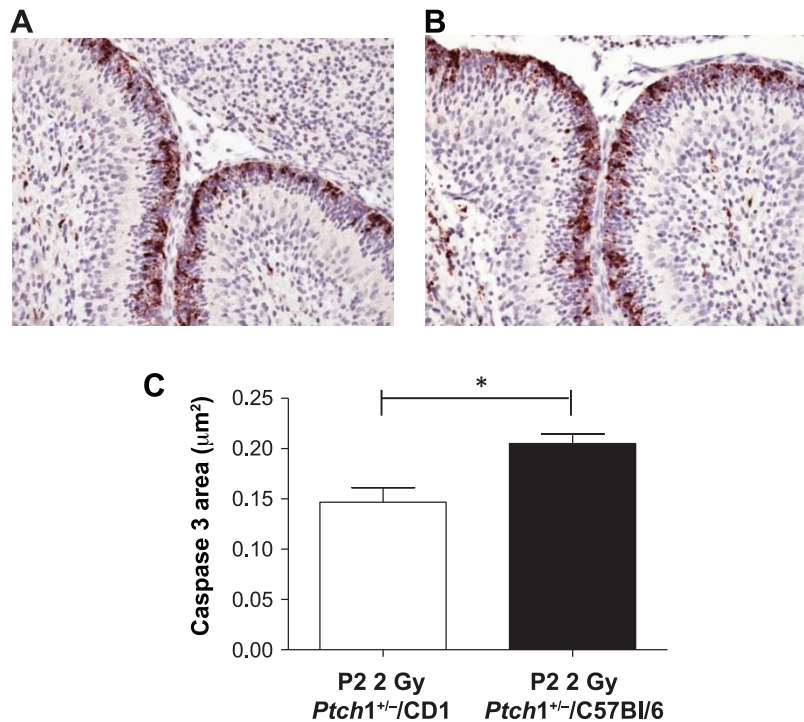


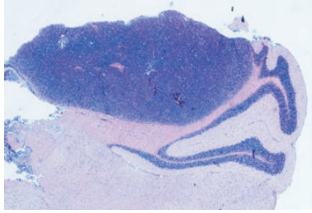
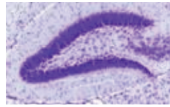
**FIG. 6.** Genetic background-dependent cell-killing differences in the cerebellum of *Ptch1*<sup>+/-</sup> mice after 2 Gy P2-irradiation using  $\gamma$  rays. Panels A and B: Representative images of apoptosis in the external granule layer of the cerebellum in *Ptch1*<sup>+/-</sup>/CD1 and *Ptch1*<sup>+/-</sup>/C57Bl/6 mice, respectively, at 4 h postirradiation, visible as caspase-3 labeling. Panel C: Quantification showing significantly higher caspase-3 staining in *Ptch1*<sup>+/-</sup>/C57Bl/6 compared to *Ptch1*<sup>+/-</sup>/CD1 mice.

<sup>DE</sup> mutation enhanced in C57Bl/6 and suppressed in CD1 have also been reported (43).

In addition to the substantial genetic variation for cancer and non-cancer diseases, genetic modifiers are known to influence the interaction of a given mutation with environmental factors, modifying the proportion of individuals affected after exposure. Therefore, we here assessed the extent to which genetic background determines variation in radiosensitivity to induction of lens opacity, brain cancer and deficits of neurogenesis in *Ptch1*<sup>+/-</sup> mutants, as clarifying genetic background interactions for multiple diseases associated with the same causative mutation may help elucidate the mechanisms underlying these diseases and radiation health risks. We demonstrated a marked dependence of both cancer and non-cancer radiation-induced pathologies on mouse genetic background, although the strain-dependent radiosensitivity was not in concord for all the three examined tissues (Fig. 7). In *Ptch1*<sup>+/-</sup> mutants, a genetic background-related inverse relationship was identified between the radiosensitivity to induction of lens opacity and MB compared to the induction of deficit of neurogenesis. In fact, high incidence of radiation-induced cataract and MB is observed in *Ptch1*<sup>+/-</sup>/CD1 mutants that instead show no consequence of radiation on neurogenesis. On the contrary, *Ptch1*<sup>+/-</sup>/C57Bl/6 mice, which are resistant to the induction of cataract and MB by radiation, are prone to the induction of neurogenesis defects,

suggesting opposite radiation responses of the lens and cerebellum compared to the DG.

From a mechanistic point of view, in the cerebellum the resistance of *Ptch1*<sup>+/-</sup>/C57Bl/6 mice to radiation-induced MB tumorigenesis, compared to *Ptch1*<sup>+/-</sup>/CD1, is associated with a high sensitivity of the neural precursors, the MB cell of origin, to the killing effect early after irradiation. This is further supported from the observation that C57Bl/6 background is not *per se* suppressive for MB, as the spontaneous MB rate in nonirradiated *Ptch1*<sup>+/-</sup>/C57Bl/6 is significantly higher than that of *Ptch1*<sup>+/-</sup>/CD1 mice, and that the abrogation is limited to radiation-induced phenomena. In strong agreement, C57Bl/6 mice are considered a radioresistant strain, and are known to develop fewer types of cancers after irradiation (44–47). Notably, DNA repair ability is very important from the radiation-response perspective, and differential repair ability can determine the degree of damage in the cells due to radiation exposure and thus its susceptibility. Accordingly, miRNome analysis of pathways associated with DNA repair function in the lens of these mice at 24 h postirradiation showed a completely different DDR, mainly mediated by a marked upregulation of p53 signaling in *Ptch1*<sup>+/-</sup>/C57Bl/6 lenses that was not detected on a CD1 background (results object of another manuscript of this special issue), suggesting different abilities to sense and respond to radiation exposure, and indicative of persistent DNA damage in irradiated C57Bl/6 mice. *In vitro* investigations comparing the radiation

	 <i>Ptch1</i> <sup>+/-</sup> /CD1	 <i>Ptch1</i> <sup>+/-</sup> /C57Bl/6
 <b>Medulloblastoma</b>	 <b>Increase</b>	<b>No induction</b>
 <b>Lens opacity</b>	 <b>Increase</b>	<b>No induction</b>
 <b>Neurogenesis defects</b>	<b>No induction</b>	 <b>Increase</b>

**FIG. 7.** Schematic representation of the dependence of *Ptch1*-associated radiation risk for lens opacity, MB development and neurogenesis defects on mouse genetic background.

response of stem cells derived from *Ptch1*<sup>+/-</sup>/C57Bl/6 and *Ptch1*<sup>+/-</sup>/CD1 mouse organs could help to unravel the basis of the genetic background-related different radiosensitivities in the two mouse strains.

Stem and progenitor cells are considered a major target of radiation-induced health effects, due to their life-long role in tissue homeostasis. Stem and progenitor cell populations are equipped with a DDR system, crucial for maintenance of genomic integrity, sensing DNA damage, arresting cell cycle, repairing DNA lesions, and/or inducing programmed cell death under extensive damage. In fact, if on one hand survival of cells with unrepaired damage might favor accumulation of genetic abnormalities increasing oncogenic risk, on the other hand, massive elimination of damaged cells can affect tissue homeostasis, compromising lineage functionality. The apparent discrepancy in the radiosensi-

tivity of the lens and cerebellum compared to that of the DG can be reconciled, considering that a stringent elimination of stem precursor cells in *Ptch1*<sup>+/-</sup>/C57Bl/6, which may prevent the induction of cataract and MB, can instead exhaust the precursors pool, impairing hippocampal neurogenesis. Conversely, *Ptch1*<sup>+/-</sup>/CD1 mice, showing a higher damage tolerance in terms of cell killing, are prone to MB and cataract induction by radiation, but are resistant to the induction of neurogenesis dysfunction in the DG. A fine balance between maintenance of tissue homeostasis and genomic stability is required to respond to radiation insult, preventing health risks. Deviation from this balance might account for the opposite strain sensitivity to radiation-induced pathologies observed in *Ptch1*<sup>+/-</sup>/C57Bl/6 and *Ptch1*<sup>+/-</sup>/CD1 mice. On the whole, although lens and brain are both radiosensitive tissues that manifest detrimental

effects even after low-dose radiation exposure, our data did not show a direct correlation between induction of lens opacity and dysfunctional hippocampal neurogenesis after irradiation, providing no support to the recent hypothesis of an eye-brain axis and to the use of ophthalmic damage as a biomarker of more generalized brain pathology (48).

A further important aspect to clarify in radiation protection is the influence of dose rate for radiation health risks. The effect of ionizing radiation on biological targets depends significantly on the particle fluence of radiation per unit of time, the so-called dose-rate effect. During protracted irradiation at lower dose rates, DNA damage repair competes with production of detrimental DNA lesions along the particle track, leading to a reduction in cell killing. We here examined the contribution of dose rate on health risk by comparing the effect of 2 Gy radiation at 0.3 or 0.063 Gy/min (irradiation time of approximately 7 min vs. 30 min) in both cancer and non-cancer pathologies, demonstrating that dose rate did not modify mouse survival, lens opacity or MB development, even in the radiosensitive CD1 mouse line. Lack of significant dose-rate effects for MB were also established at lower radiation doses of 0.5 Gy and 1 Gy.

Another important consideration raised by our findings is the extent to which the individual differences, here represented by genetic background hosting the *Ptch1* mutation, determine a phenotypic variation in the relationship between dose and disease risk. Data for cancer effects constitute a proof of principle that genetic background largely influences the dose dependence of radiation effects: 0.5 Gy significantly increases MB incidence in *Ptch1*<sup>+/-</sup>/CD1 mice, while 2 Gy radiation does not raise the incidence of MB above the spontaneous rate in *Ptch1*<sup>+/-</sup>/C57/Bl6 mice. This huge variation in individual risk can dramatically affect the risk estimates, especially at low doses, and also has important implications for dose limits in the population.

The central aim of radiological protection is to preserve human health from harmful radiation effects. Experimental mouse studies are important to gain a comprehensive, quantitative and mechanistic understanding of the biological factors that modify individual risk of radiation-induced health effects, including age at exposure, dose, dose rate, organ/tissue specificity and genetic factors. Concerns regarding the variation of radiation risk among individuals for cancer and, importantly, for the less investigated non-cancer diseases, present important ethical and policy questions for current system and regulations. Developing models of radiation-induced disease pathogenesis that account for individual risk factors is important to unravel individual sensitivity and may help to refine radiation protection system. Mechanistic understanding of radiation-induced disease processes provided here allow for further insights into the genetic basis of radiation sensitivity in three different, highly organized and differentiated tissues, in a mouse model of great relevance to radiation response in humans. The significant phenotypic differences in radiation response occurring when the *Ptch1* mutation is hosted in a C57Bl/6 or CD1 background may be

suitable for a genetic modifier screen aimed at identifying interacting genes responsible for this difference, which may also be relevant for humans.

In summary, our results demonstrate a critical dependence of cancer and non-cancer radiation-induced diseases on the genetic background, which significantly modulates induction of MB and occurrence of neurogenesis alterations, and can even abrogate the predisposition to radiogenic lens opacity conferred by the *Ptch1* mutation, which represents a paradigm of radiation hypersensitivity. Altogether, our findings point to a dominant role of genetic risk modifiers in controlling both early and late radiation-induced tissue responses. These findings have important implications for radiosensitive subsets of the human population, especially in the context of individuals exposed to radiation in occupational or medical situations. By taking into account individual genetic variability, as well as the effect of radiation dose and dose rate, these findings are also relevant for the development of guidelines for occupational and therapeutic radiation exposure.

#### ACKNOWLEDGMENTS

This study was supported by the LDLensRad Project, which has received funding from the Euratom Research and Training Programme 2014–2018, in the framework of the CONCERT EJP (grant agreement no. 662287). This article reflects only the authors' view. Responsibility for the information and views expressed herein lie entirely with the authors. The European Commission is not responsible for any use that may be made of the information it contains. This work was also partially supported by the Fondazione AIRC per la Ricerca sul Cancro (NANOCROSS project; grant no. 20314 to MM) We thank Dr. Maria Pimpinella and Ms. Vanessa De Coste for dosimetry and irradiation. This study is dedicated to the memory of Gabriele Babini, who passed away suddenly on November 5, 2020.

Received: November 4, 2020; accepted: March 19, 2021; published online: April 15, 2021

#### REFERENCES

1. Hamada N, Fujimichi Y, Iwasaki T, Fujii N, Furuhashi M, Kubo E, et al. Emerging issues in radiogenic cataracts and cardiovascular disease. *J Radiat Res* 2014; 55:831-46.
2. Armstrong, GT, Jain, N, Liu, W, Merchant, TE, Stovall M, Srivastava DK. Region-specific radiotherapy and neuropsychological outcomes in adult survivors of childhood CNS malignancies. *Neuro Oncol* 2010; 12:1173-86.
3. de Ruiter MA, van Mourik R, Schouten-van Meeteren AY, Grootenhuys MA, Oosterlaan J. Neurocognitive consequences of a paediatric brain tumour and its treatment: a meta-analysis. *Dev Med Child Neurol* 2013; 55:408-17.
4. Mulhern RK, Merchant TE, Gajjar A, Reddick WE, Kun LE. Late neurocognitive sequelae in survivors of brain tumours in childhood. *Lancet Oncol* 2004; 5:399-408.
5. Bouffler S, Auvinen A, Cardis E, Durante M, Jourdain JR, Harms-Ringdahl M, et al. Strategic research agenda of the Multidisciplinary European Low Dose Initiative (MELODI) – 2019. (<https://bit.ly/2NRTL4p>)
6. National Research Council. Health risks from exposure to low levels of ionizing radiation: BEIR VII phase 2. Washington, DC: National Academies Press; 2006.
7. Cavodeassi F, Creuzet S, Etchevers HC. The hedgehog pathway and ocular developmental anomalies. *Hum Genet* 2019; 138:917-36.

8. Kerr CL, Huang J, Williams, T, West-Mays JA. Activation of the hedgehog signaling pathway in the developing lens stimulates ectopic FoxE3 expression and disruption in fiber cell differentiation. *Invest Ophthalmol Vis Sci* 2012; 53:3316–30.
9. Tsonis PA, Vergara MN, Spence JR, Madhavan M, Kramer EL, Call MK, et al. Novel role of the hedgehog pathway in lens regeneration. *Dev Biol* 2004; 267:450–61.
10. Vaillant C, Monard D. SHH pathway and cerebellar development. *Cerebellum* 2009; 8:291–301.
11. McMahon AP, Ingham PW, and Tabin CJ. Developmental roles and clinical significance of hedgehog signaling. *Curr Top Dev Biol* 2003; 53:1–114.
12. Han YG, Spassky N, Romaguera-Ros M, Garcia-Verdugo JM, Aguilar A, Schneider-Maunoury S, et al. Hedgehog signaling and primary cilia are required for the formation of adult neural stem cells. *Nat Neurosci* 2008; 11:277–84.
13. Breunig JJ, Sarkisian MR, Arellano JI, Morozov YM, Ayoub AE, Sojitra S, et al. Primary cilia regulate hippocampal neurogenesis by mediating sonic hedgehog signaling. *Proc Natl Acad Sci U S A* 2008; 105:13127–32.
14. Chen JJ, Sartori J, Aakalu VK, Setabutr P. Review of ocular manifestations of nevoid basal cell carcinoma syndrome: What an ophthalmologist needs to know. *Middle East Afr J Ophthalmol* 2015; 22:421–7.
15. Jen M, Nallasamy S. Ocular manifestations of genetic skin disorders. *Clin Dermatol* 2016; 34:242–75
16. Goodrich LV, Milenkovic L, Higgins KM, Scott MP. Altered neural cell fates and medulloblastoma in mouse patched mutants. *Science* 1997; 277:1109–13.
17. Hahn H, Wojnowski L, Zimmer AM, Hall J, Miller G, Zimmer A. Rhabdomyosarcomas and radiation hypersensitivity in a mouse model of Gorlin syndrome. *Nat Med* 1998; 4:619–22
18. Jackson TW, Bendfeldt GA, Beam KA, Rock KD, Belcher SM. Heterozygous mutation of sonic hedgehog receptor (Ptc1) drives cerebellar overgrowth and sex-specifically alters hippocampal and cortical layer structure, activity, and social behavior in female mice. *Neurotoxicol Teratol* 2020; 78:106866.
19. Antonelli F, Casciati A, Tanori M, Tanno B, Linares-Vidal MV, Serra N, et al. Alterations in morphology and adult neurogenesis in the dentate gyrus of Patched1 heterozygous mice. *Front Mol Neurosci* 2018; 23:11–168.
20. Pazzaglia S, Mancuso M, Atkinson MJ, Tanori M, Rebessi S, Majo VD, et al. High incidence of medulloblastoma following X-ray-irradiation of newborn Ptc1 heterozygous mice. *Oncogene* 2002; 21:7580–4
21. Mancuso M, Pazzaglia S, Tanori M, Hahn H, Merola P, Rebessi S, et al. Basal cell carcinoma and its development: insights from radiation-induced tumors in Ptc1-deficient mice. *Cancer Res* 2004; 64:934–41
22. De Stefano I, Tanno B, Giardullo P, Leonardi S, Pasquali E, Antonelli F, et al. The Patched 1 tumor-suppressor gene protects the mouse lens from spontaneous and radiation-induced cataract. *Am J Pathol* 2015; 185:85–95.
23. De Stefano I, Giardullo P, Tanno B, Leonardi S, Pasquali E, Babini G, et al. Nonlinear radiation-induced cataract using the radiosensitive Ptc1(+/-) mouse model. *Radiat Res* 2016; 186:315–21.
24. Hahn H, Wojnowski L, Specht K, Kappler R, Calzada-Wack J, Potter D, et al. Patched target Igf2 is indispensable for the formation of medulloblastoma and rhabdomyosarcoma. *J Biol Chem* 2000; 275:28341–4.
25. Puk O, de Angelis MH, Graw J. Lens density tracking in mice by Scheimpflug imaging. *Mamm Genome* 2013; 24:295–302.
26. Casciati A, Dobos K, Antonelli F, Benedek A, Kempf SJ, Belles M, et al. Age-related effects of X-ray irradiation on mouse hippocampus. *Oncotarget* 2016; 10:28040–8.
27. Mancuso M, Giardullo P, Leonardi S, Pasquali E, Casciati A, De Stefano I, et al. Dose and spatial effects in long-distance radiation signaling in vivo: implications for abscopal tumorigenesis. *Int J Radiat Oncol Biol Phys* 2013; 85:813–9.
28. Shiels A, Hejtmancik JF. Mutations and mechanisms in congenital and age-related cataracts. *Exp Eye Res* 2017; 156:95–102
29. Pei X, Bao Y, Chen Y, Li X. Correlation of lens density measured using the Pentacam Scheimpflug system with the Lens Opacities Classification System III grading score and visual acuity in age-related nuclear cataract. *Br J Ophthalmol* 2008; 92:1471–5.
30. Altman J, Das GD. Autoradiographic and histological evidence of postnatal hippocampal neurogenesis in rats. *J Comp Neurol* 1965; 124:319–35.
31. Greene-Schloesser D, Moore E, Robbins ME. Molecular pathways: Radiation-induced cognitive impairment. *Clin Cancer Res* 2013; 19:2294–300.
32. Monje M, Dietrich J. Cognitive side effects of cancer therapy demonstrate a functional role for adult neurogenesis. *Behav Brain Res* 2012; 227:376–9.
33. Ji S, Tian Y, Lu Y, Sun R, Ji J, Zhang L, et al. Irradiation-induced hippocampal neurogenesis impairment is associated with epigenetic regulation of bdnf gene transcription. *Brain Res* 2014; 1577:77–88.
34. Foray N, Bourguignon M, Hamada N. Individual response to ionizing radiation. *Mutat Res* 2016; 770:369–86.
35. Calzada-Wack J, Kappler R, Schnitzbauer U, Richter T, Nathrath M, Rosemann M, et al. Unbalanced overexpression of the mutant allele in murine Patched mutants. *Carcinogenesis* 2002; 23:727–33.
36. Pazzaglia S, Mancuso M, Tanori M, Atkinson MJ, Merola P, Rebessi S, et al. Modulation of patched-associated susceptibility to radiation induced tumorigenesis by genetic background. *Cancer Res* 2004; 64:3798–806
37. Pazzaglia S. Ptc1 heterozygous knockout mice as a model of multi-organ tumorigenesis. *Cancer Lett* 2006; 234:124–34.
38. McCarty CA, Taylor HR. The genetics of cataract. *Invest Ophthalmol Vis Sci* 2001; 42:1677–8.
39. Hammond CJ, Duncan DD, Snieder H, de Lange M, West SK, Spector TD, et al. The heritability of age-related cortical cataract: the twin eye study. *Invest Ophthalmol Vis Sci* 2001; 42:601–5.
40. Hammond CJ, Snieder H, Spector TD, Gilbert CE. Genetic and environmental factors in age-related nuclear cataracts in monozygotic and dizygotic twins. *N Engl J Med* 2000; 342:1786–90.
41. Kempermann G, Chesler EJ, Lu L, Williams RW, Gage FH. Natural variation and genetic covariance in adult hippocampal neurogenesis. *Proc Natl Acad Sci U S A* 2006; 103:780–5
42. Tylzanowski P, Mebis L, Luyten FP. The Noggin null mouse phenotype is strain dependent and haploinsufficiency leads to skeletal defects. *Dev Dyn*. 2006; 235:1599–607.
43. Tanabe LM, Martin C, Dauer WT. Genetic background modulates the phenotype of a mouse model of DYT1 dystonia. *PLoS One* 2012; 7:e32245.
44. Kataoka T, Mizuguchi Y, Notohara K, Taguchi T, Yamaoka K. Histological changes in spleens of radiosensitive and radioresistant mice exposed to low-dose X-ray irradiation. *Physiol Chem Phys Med NMR* 2006; 38:21–9.
45. Mills CD, Kincaid K, Alt JM, Heilman MJ, Hill AM. M-1/M-2 Macrophages and the Th1/Th2 paradigm. *J Immunol* 2000; 164:6166–73.
46. Okayasu R, Suatomi K, Yu Y, Silver A, Bedford JS, Cox R, et al. A deficiency in DNA repair and DNA-PKcs expression in the radiosensitive BALB/c mouse. *Cancer Res* 2000; 60:4342–5.
47. Storer JB, Mitchell TJ, Fry RJ. Extrapolation of the relative risk of radiogenic neoplasms across mouse strains and to man. *Radiat Res* 1988; 114:331–53
48. Loganovsky KN, Marazziti D, Fedirko PA, Kuts KV, Antypchuk KY, Perchuk IV, et al. Radiation-induced cerebro-ophthalmic effects in humans. *Life (Basel)* 2020; 10:41.